Supplementary Information

Thermodynamic Phase Control of Cu-Sn Alloy Electrocatalysts for Selective CO_2 Reduction

Soohyun Go[1,†], Woosuck Kwon[1,†], Deokgi Hong[2,†], Taemin Lee[1], Sang-Ho Oh[2], Daewon Bae[1], Jeong-Heon Kim[1], Seolha Lim[1], Young-Chang Joo[2], and Dae-Hyun Nam[1,3,*]

[1]*Department of Energy Science and Engineering, Daegu Gyeongbuk Institute of Science and Technology (DGIST), Daegu 42988, Republic of Korea*

[2]*Department of Materials Science and Engineering, Seoul National University, Seoul 08826, Republic of Korea*

[3]*Department of Materials Science and Engineering, Korea University, Seoul 02841, Republic of Korea*

[†]These authors contributed equally to this work.

*Corresponding author

Prof. Dae-Hyun Nam

Department of Energy Science & Engineering

Daegu Gyeongbuk Institute of Science & Technology (DGIST)

Department of Materials Science and Engineering

Korea University

E-mail: dnam@korea.ac.kr

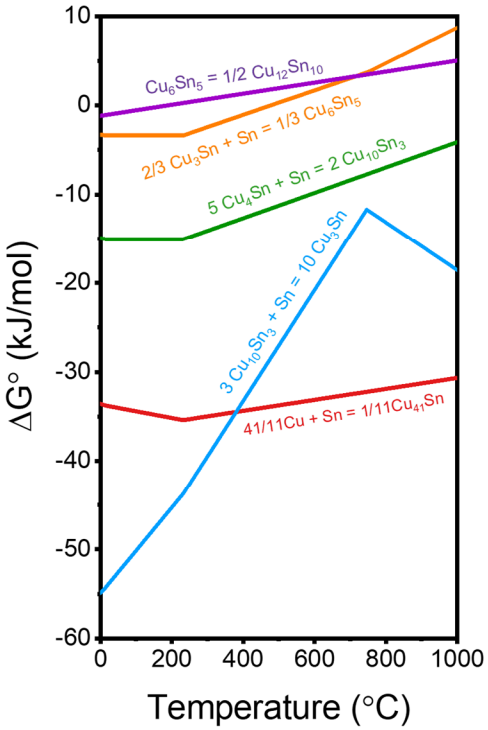

Figure S1. The standard Gibbs free energy diagram of Cu-Sn alloys.

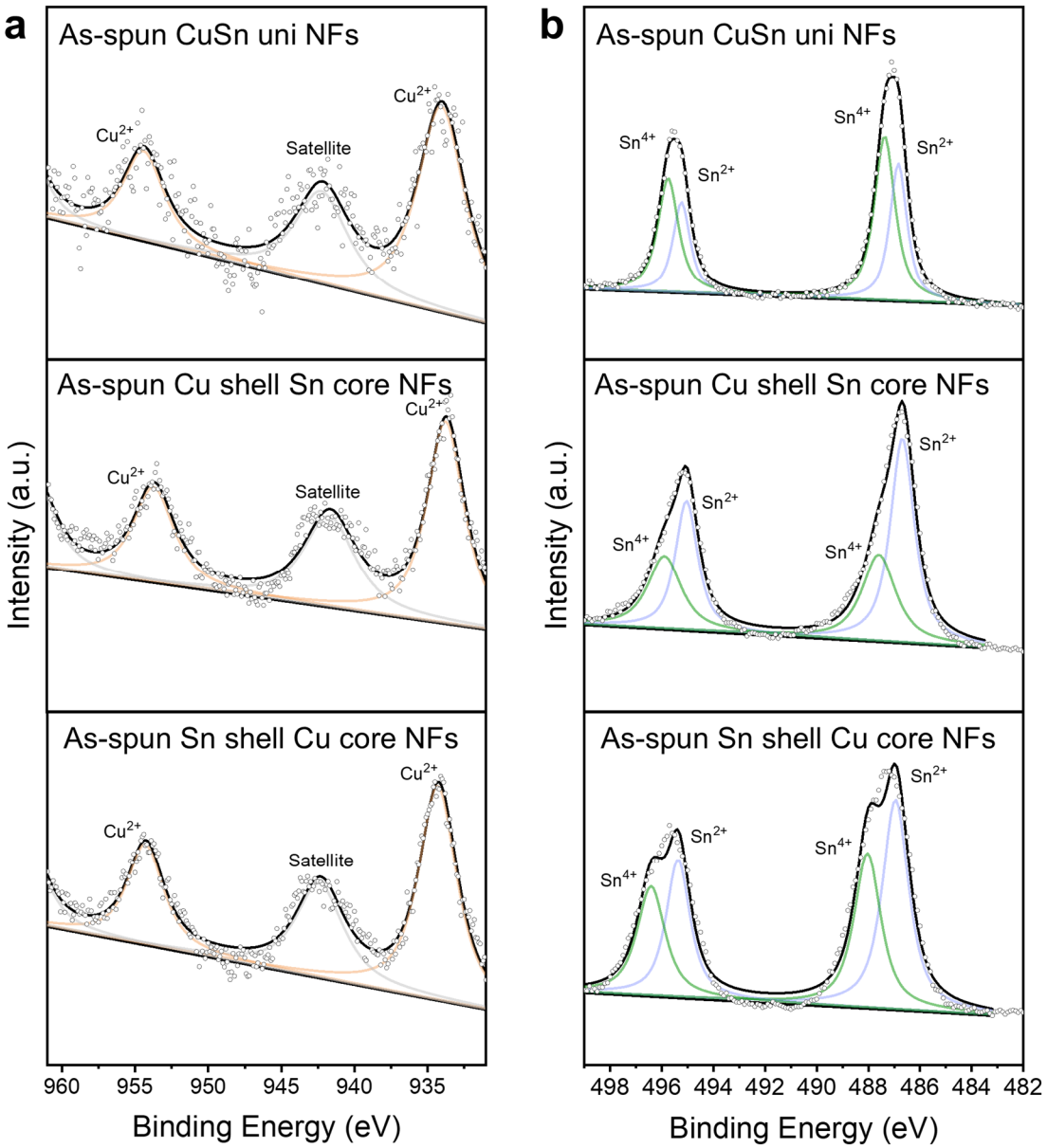

Figure S2. The XPS spectrums of as-spun CuSn uniaxial NFs, Cu shell Sn core NFs, and Sn shell Cu core NFs in terms of (a) Cu 2p and (b) Sn 3d to investigate the chemical state of as-spun NFs before the calcination. The Cu 2p peaks were deconvoluted as Cu^{+}/Cu^{0} (~933.4 eV and 953.5 eV) and Cu^{2+} (~934.5 eV and ~956 eV). The Sn 3d peaks were deconvoluted as Sn^{0} (~485.5 eV and ~493.7 eV), Sn^{2+} (~487 eV and ~495.3 eV), and Sn^{4+} (~487.9 eV and ~496 eV).[1]

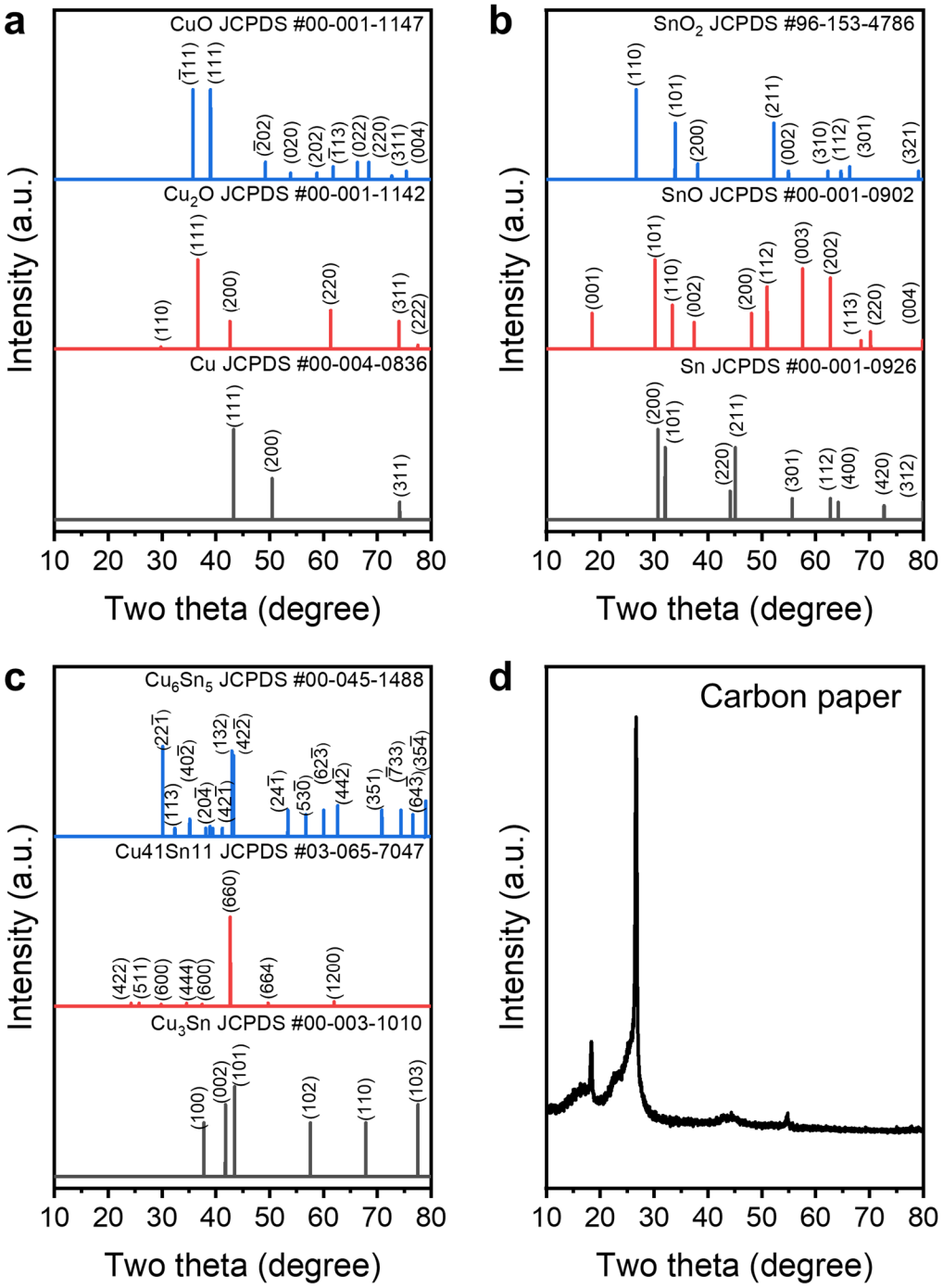

Figure S3. The XRD Pattern references of Cu, Sn oxide, metallic Cu, Sn, Cu-Sn alloys, and carbon paper. (a) The references of Cu, Cu_2O, and CuO. (b) The references of Sn, SnO, SnO_2. (c) The references of Cu_3Sn, $Cu_{41}Sn_{11}$, and Cu_6Sn_5. (d) The reference of carbon paper.

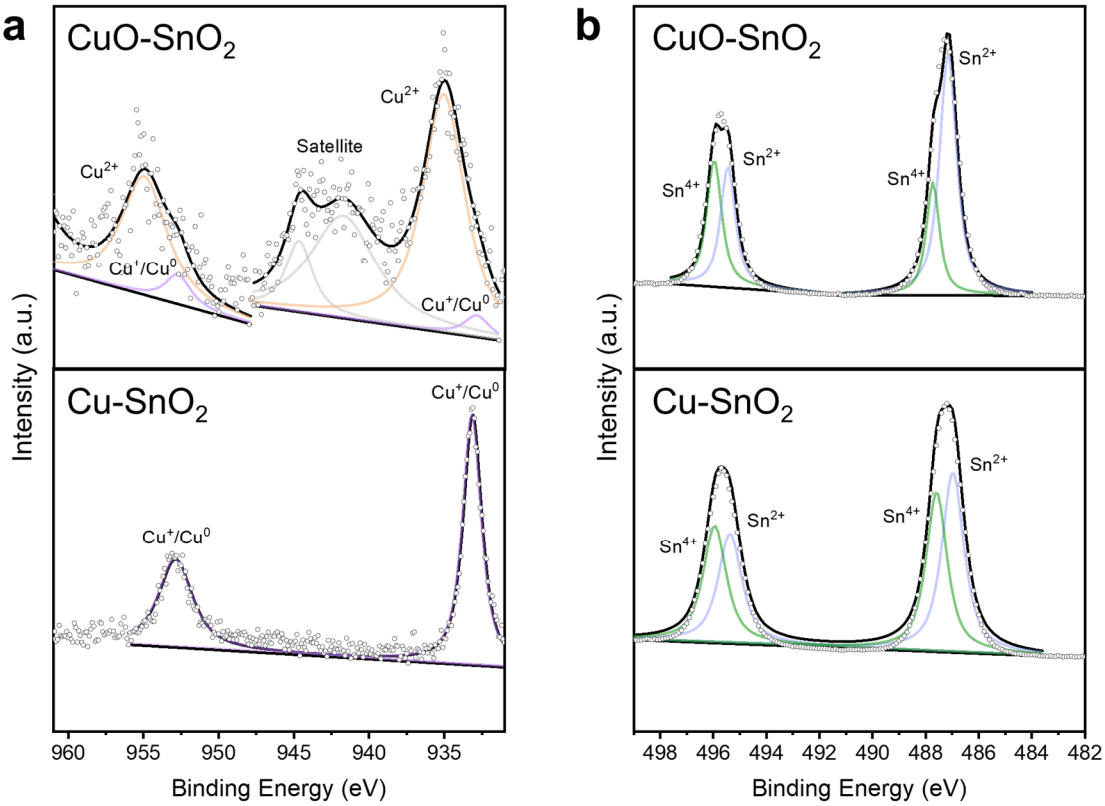

Figure S4. The XPS spectrum of Cu-Sn oxides NFs before CO_2RR to identify the oxidation state in terms of (a) Cu 2p and (b) Sn 3d. The Cu 2p peaks were deconvoluted as Cu^{+}/Cu^{0} (~933.4 eV and 953.5 eV) and Cu^{2+} (~934.5 eV and ~956 eV). Sn^{0} (~485.5 eV and ~493.7 eV), Sn^{2+} (~487 eV and ~495.3 eV), and Sn^{4+} (~487.9 eV and ~496 eV).[1] Ar etching was conducted to eliminate the native oxide layer before analysis.

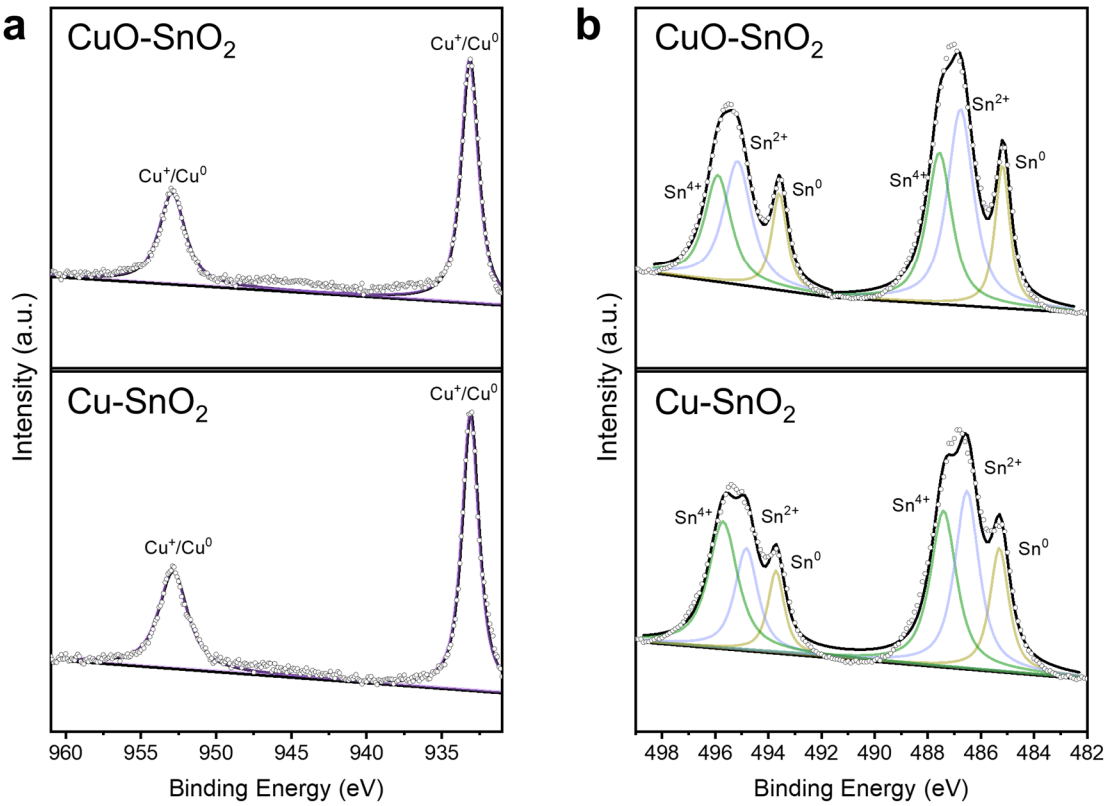

Figure S5. The XPS spectrum of Cu-Sn oxides NFs after CO_2RR to identify the oxidation state in terms of (a) Cu 2p and (b) Sn 3d. The Cu 2p peaks were deconvoluted as Cu^{+}/Cu^{0} (~933.4 eV and 953.5 eV) and Cu^{2+} (~934.5 eV and ~956 eV). Sn^{0} (~485.5 eV and ~493.7 eV), Sn^{2+} (~487 eV and ~495.3 eV), and Sn^{4+} (~487.9 eV and ~496 eV).[1] Ar etching was conducted to eliminate the native oxide layer before analysis.

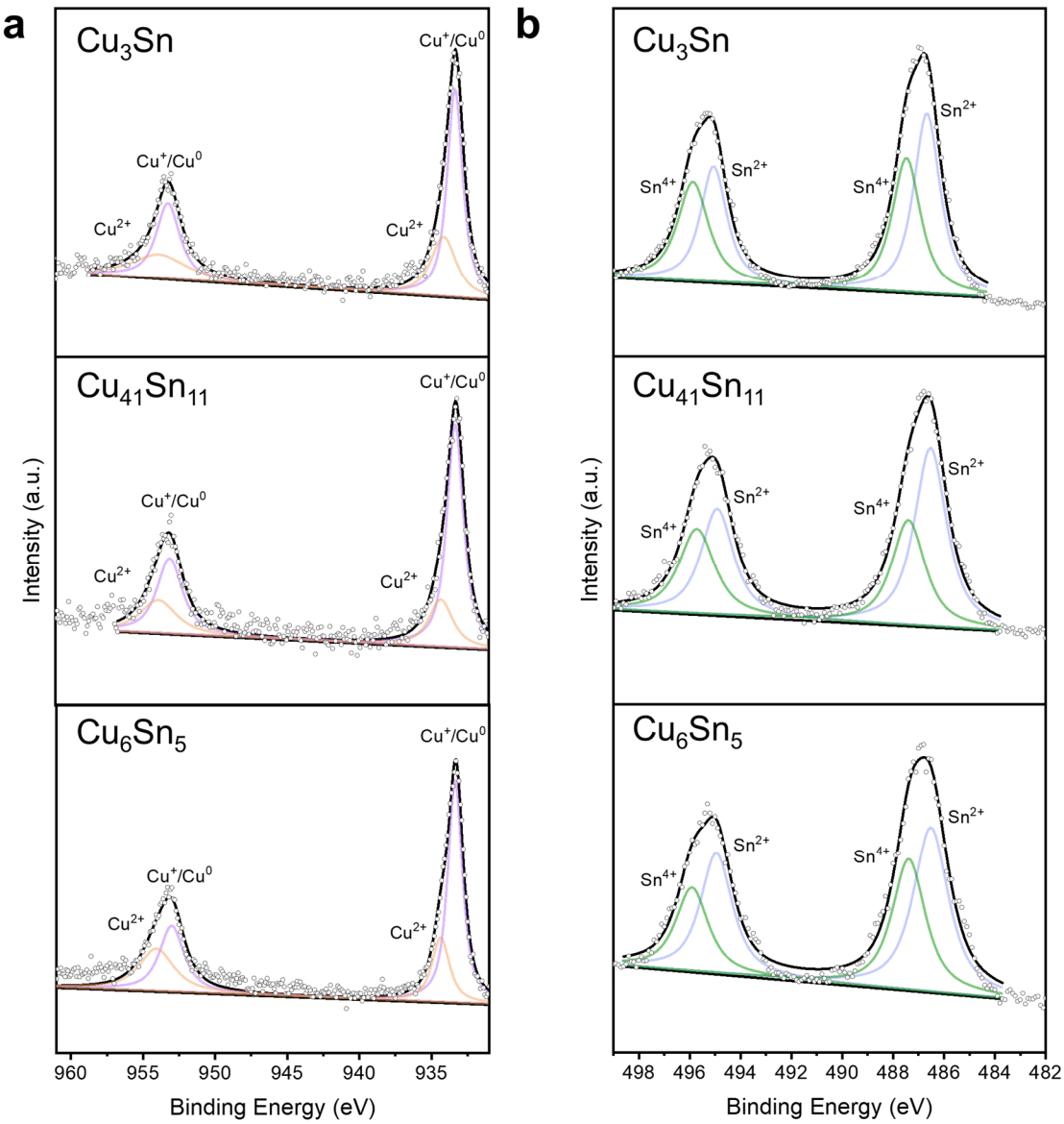

Figure S6. The XPS spectrum of Cu-Sn alloys/CNFs after CO_2RR to identify the oxidation state in terms of (a) Cu 2p and (b) Sn 3d. The Cu 2p peaks were deconvoluted as Cu^{+}/Cu^{0} (~933.4 eV and 953.5 eV) and Cu^{2+} (~934.5 eV and ~956 eV). Sn^{0} (~485.5 eV and ~493.7 eV), Sn^{2+} (~487 eV and ~495.3 eV), and Sn^{4+} (~487.9 eV and ~496 eV).[1] Ar etching was conducted to eliminate the native oxide layer before analysis.

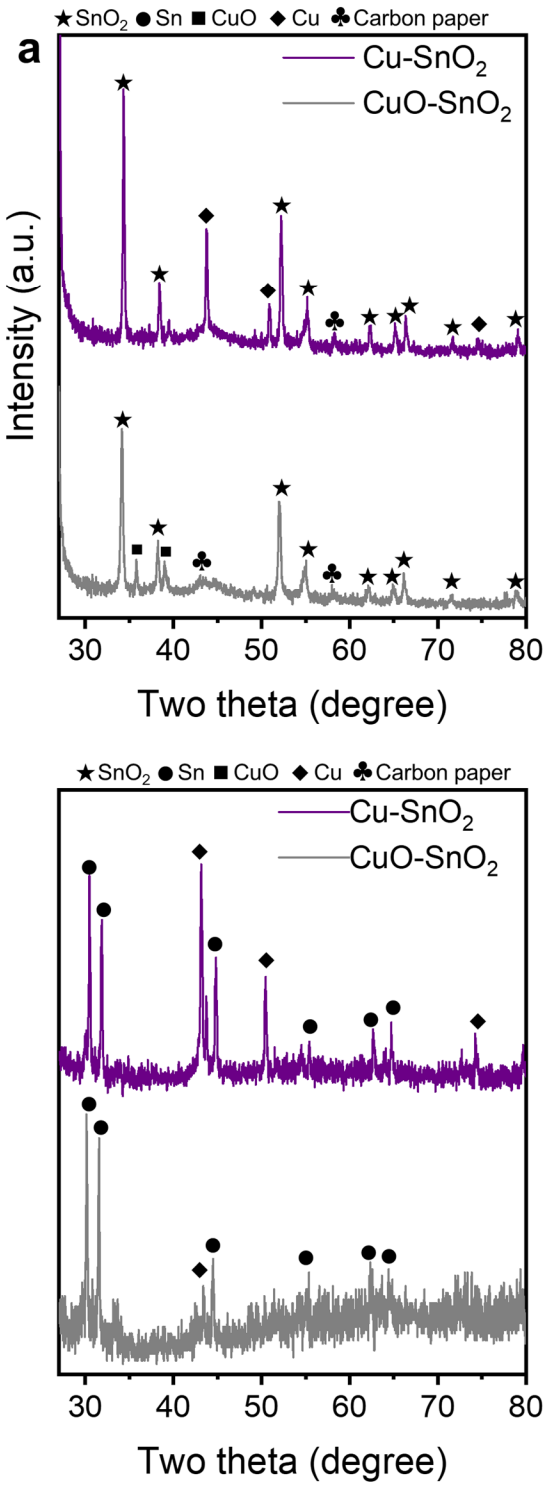

Figure S7. The XRD patterns of Cu-Sn oxides NFs on carbon paper GDL. (a) Before CO_2RR. (b) After CO_2RR.

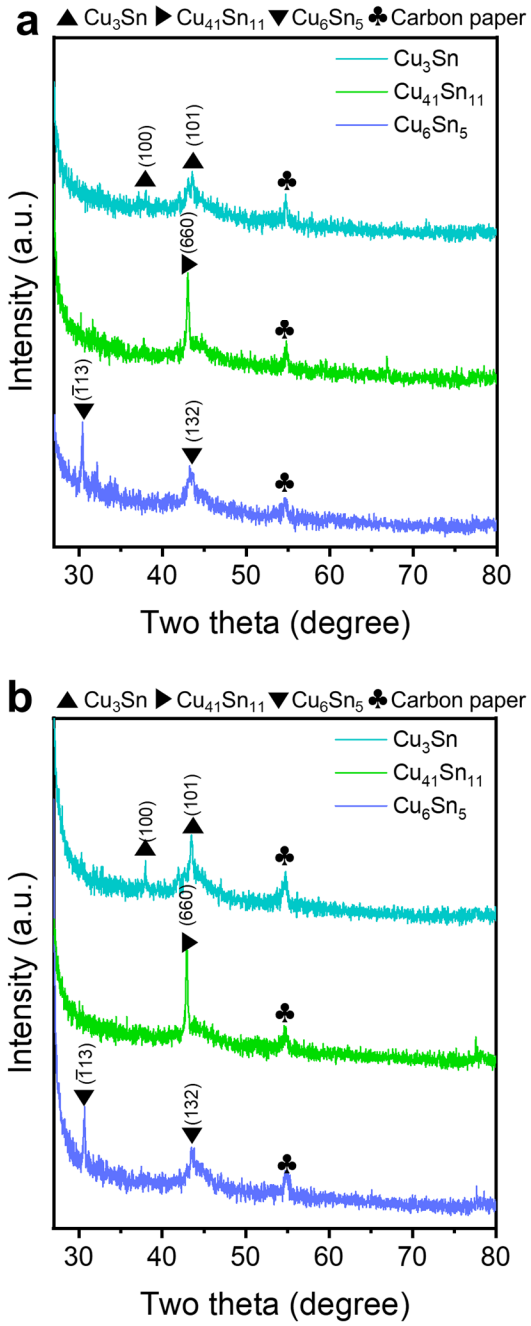

Figure S8. The XRD patterns of Cu-Sn alloys/CNFs on carbon paper GDL. (a) Before CO_2RR. (b) After CO_2RR.

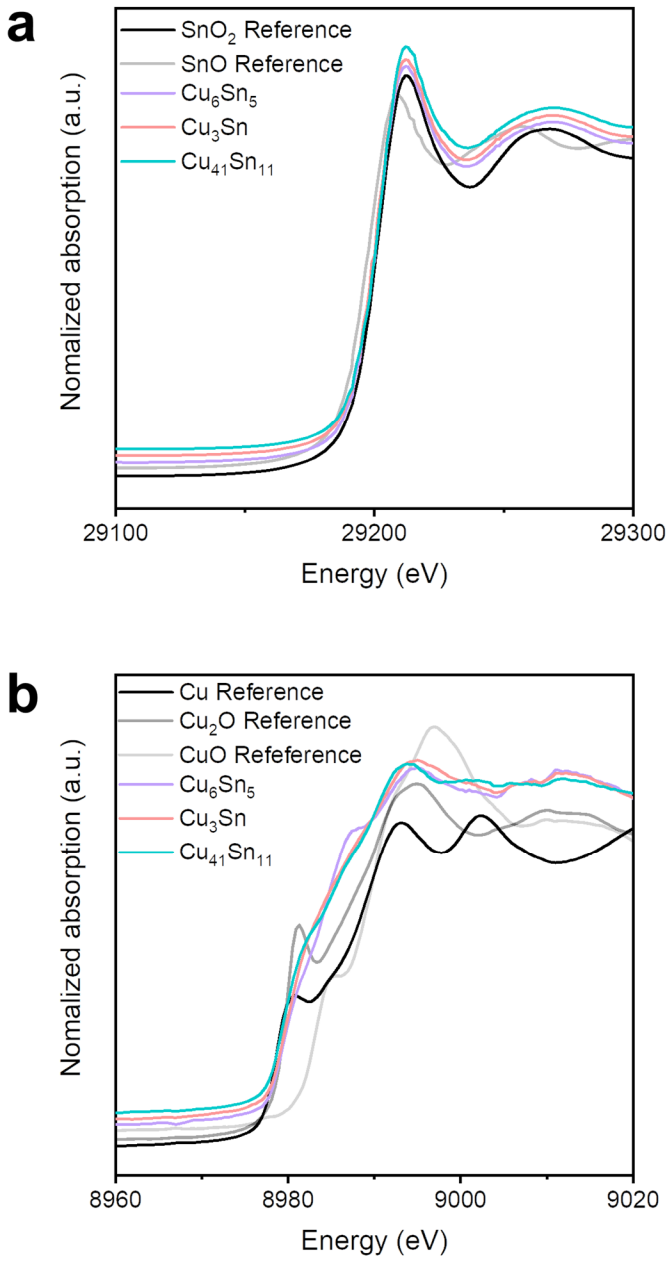

Figure S9. (a) XANES spectra at Sn-K edge for Cu_3Sn/CNFs, $Cu_{41}Sn_{11}$/CNFs, Cu_6Sn_5/CNFs, and reference SnO, SnO_2. (b) XANES spectra at Cu-K edge for Cu_3Sn/CNFs, $Cu_{41}Sn_{11}$/CNFs, Cu_6Sn_5/CNFs, and reference Cu, CuO, Cu_2O.

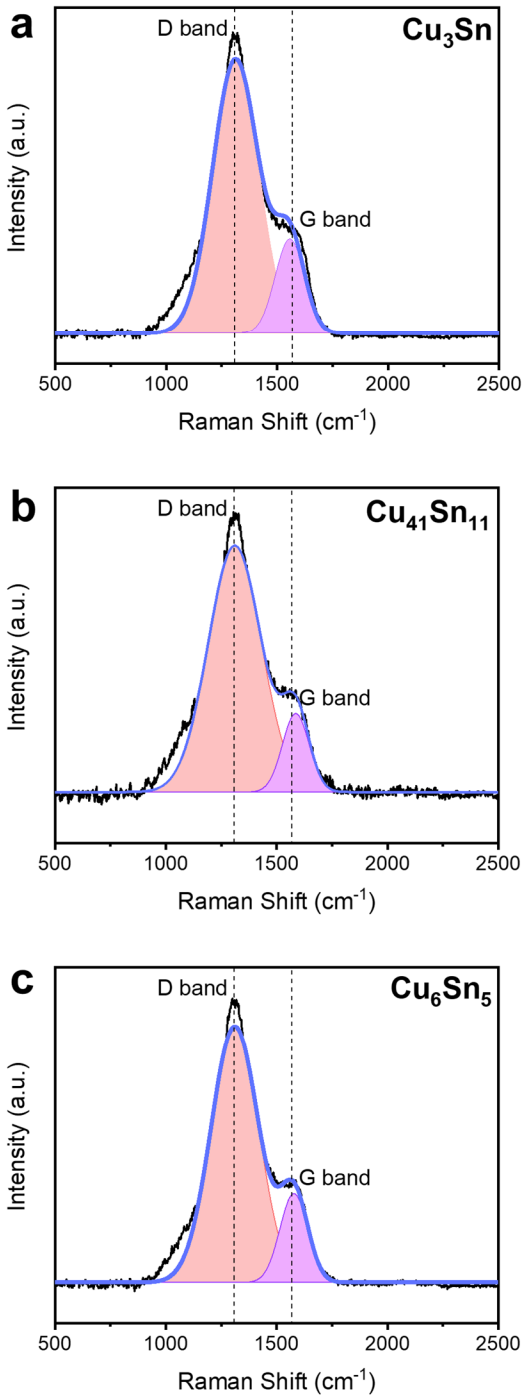

Figure S10. Bonding characteristics of carbon support. Carbon crystallinity of Cu-Sn alloy embedded nanofibers was investigated by Raman spectroscopy (a) Cu_3Sn, (b) $Cu_{41}Sn_{11}$, (c) Cu_6Sn_5. The G-band represents the planar configuration sp^2 bonded carbon (rings and chain), and the D-band is the breathing mode of sp^2 atoms (rings) directly proportional to the level of defects in the sample. Carbon crystallinity was calculated by peak intensity ratio (I_D/I_G).

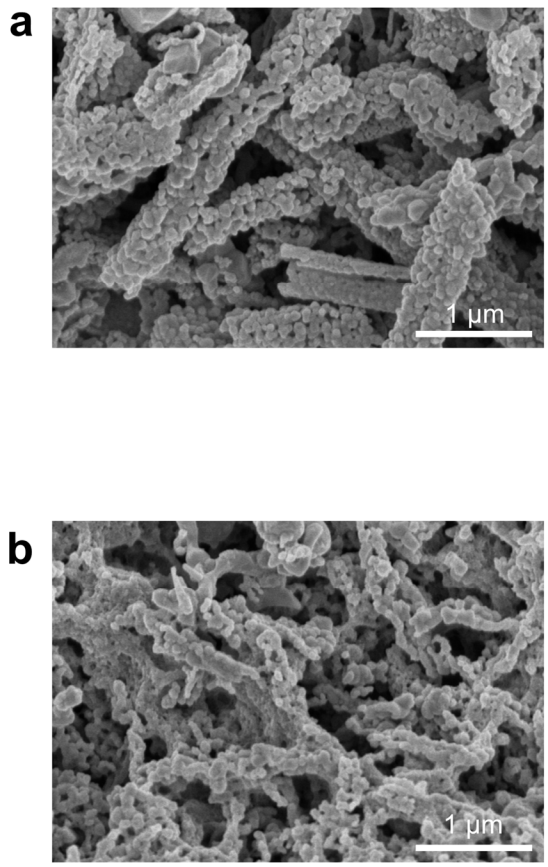

Figure S11. The SEM images of Cu-Sn oxides NFs. (a)CuO-SnO_2 NFs (b) Cu-SnO_2 NFs.

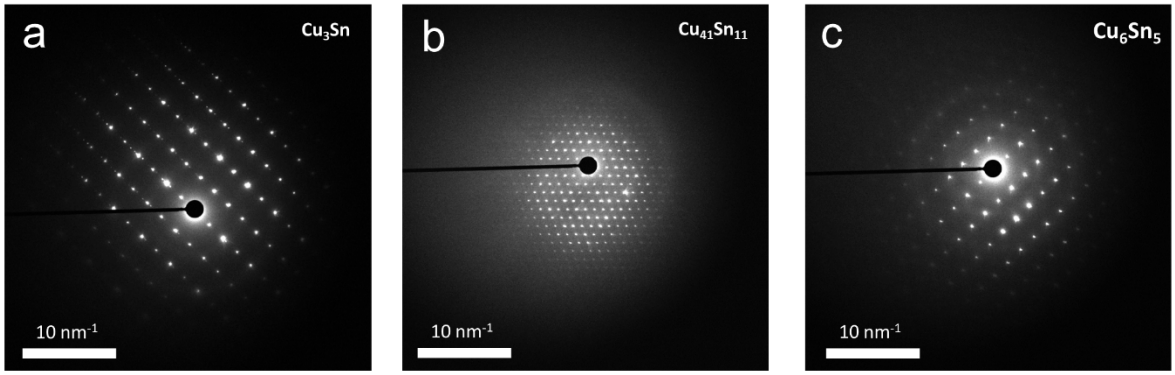

Figure S12. TEM SAED analysis (scale bar 10 nm^{-1}) results of (a) Cu_3Sn, (b) $Cu_{41}Sn_{11}$, and (c) Cu_6Sn_5 in Cu-Sn alloy/CNFs.

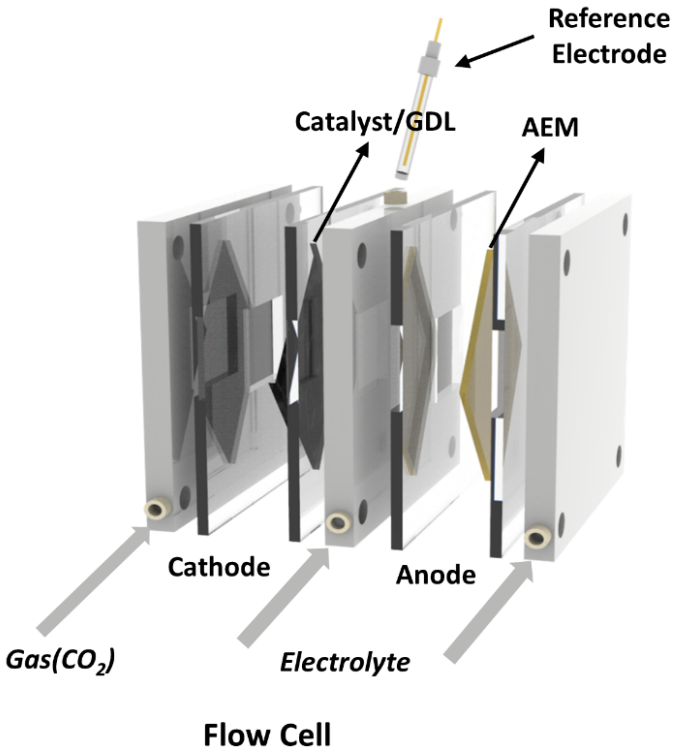

Figure S13. Schematic of flow cell composed of cathode for CO_2RR, anode, reference electrode, and anion exchange membrane

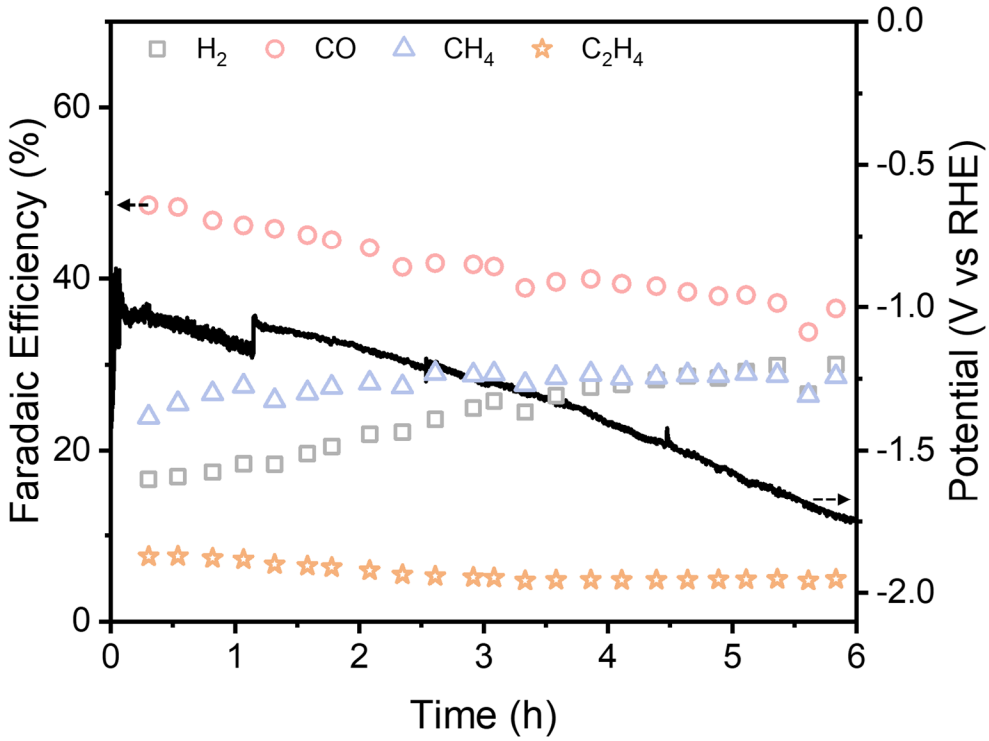

Figure S14. The CO_2RR stability of $Cu_{41}Sn_{11}$/CNFs in flow cell with 1 M KOH electrolyte at a total current of 300 mA/cm^2. The gray, pink, blue, and orange mark indicate the H_2, CO, CH_4, and C_2H_4 respectively. H_2 FE gradually increased over 30% because of low hydrophobicity of carbon paper.

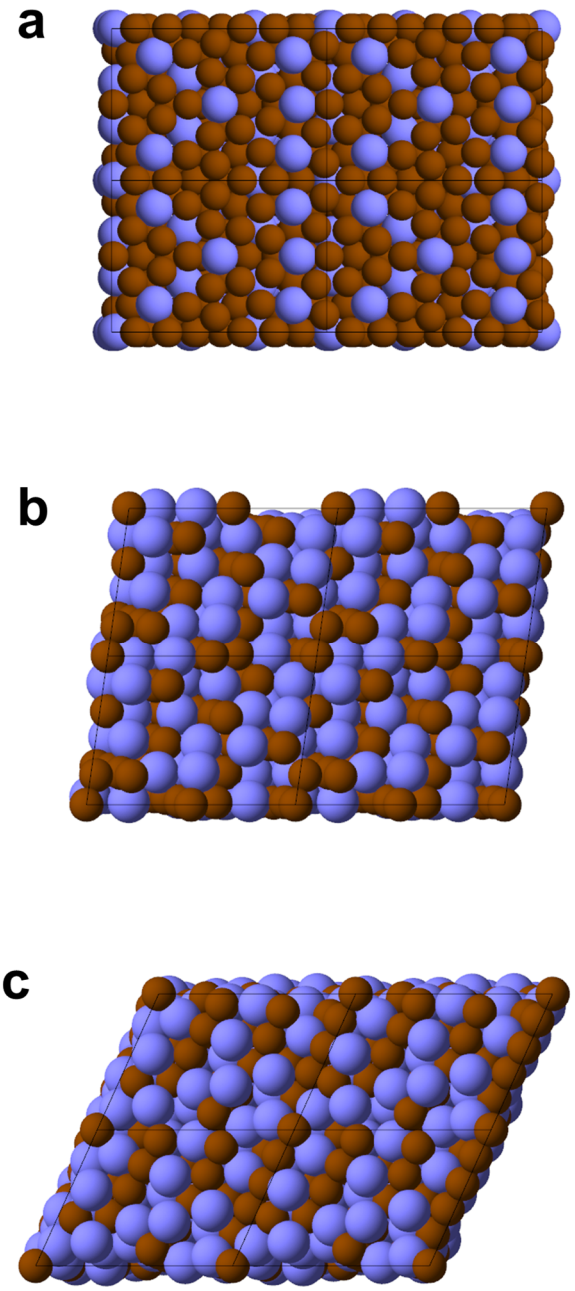

Figure S15. Atomic structure of 2×2 superecell for (a) $Cu_{41}Sn_{11}$ (660), (b) Cu_6Sn_5 (132), and (c) Cu_6Sn_5 ($\bar{1}13$) surface. Brown and blue spheres represent Cu and Sn atoms, respectively.

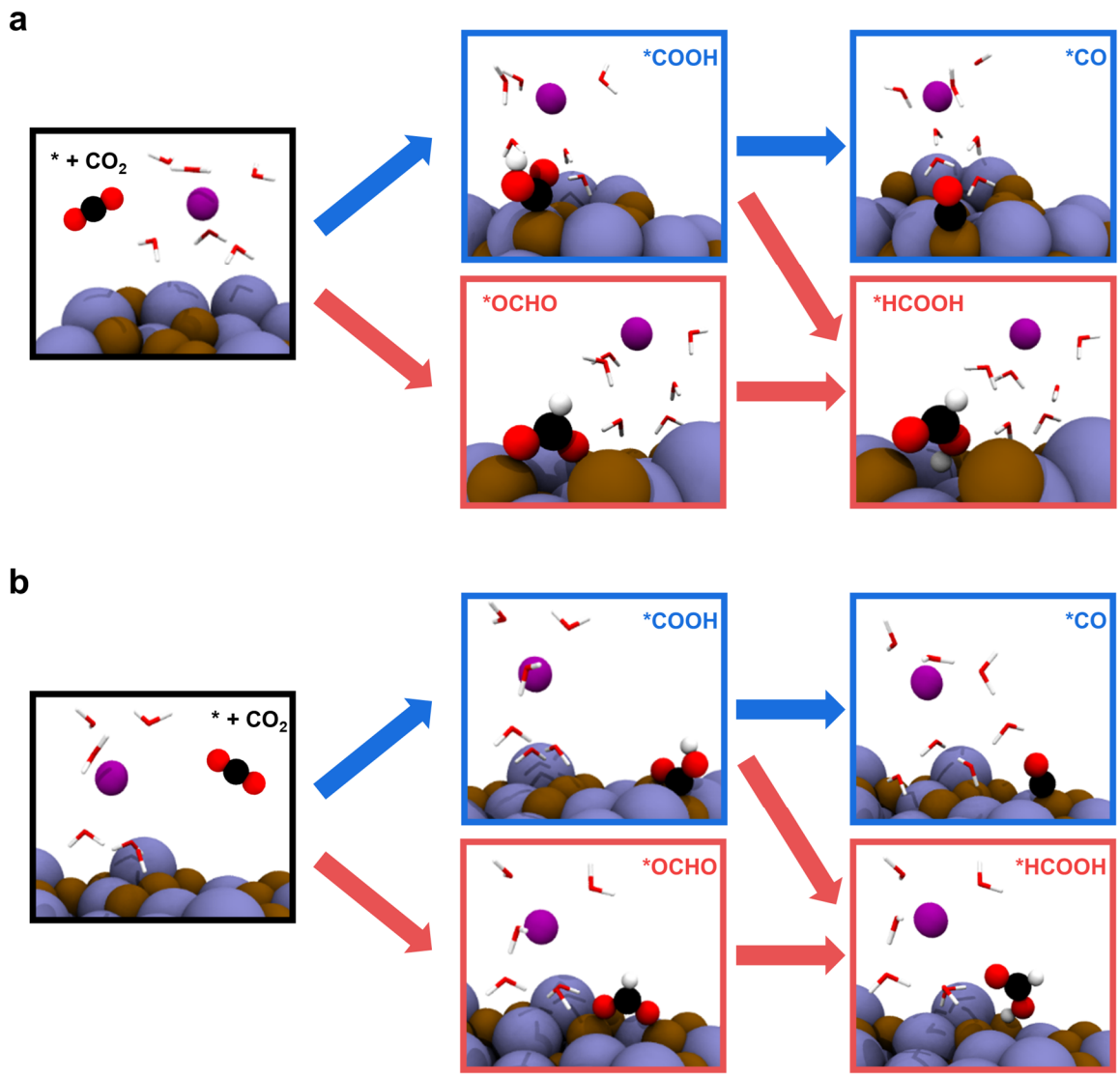

Figure S16. Atomic structure change in CO_2 reduction to *CO and *HCOOH on (a) Cu_6Sn_5 (132) and (b) Cu_6Sn_5 ($\bar{1}13$) surface. Brown, blue, black, red, white, and purple spheres represent Cu, Sn, C, O, H, and K atoms, respectively. H_2O molecules are shown as lines for brevity.

Table S1. The Cu and Sn composition of Cu-Sn alloys/CNFs acquired by inductively coupled plasma optical emission spectroscopy (ICP-OES) analysis.

Sample	Sn (ppm)	Cu (ppm)	Sn (mmol)	Cu (mmol)	Cu Sn ratio
Cu_3Sn CNFs	1.166	1.248	9.822	19.63	$Cu_{1.999}Sn$ (Cu_2Sn)
Cu_6Sn_5 CNFs	1.851	1.395	15.59	21.95	$Cu_{1.408}Sn$ (Cu_6Sn_5)
$Cu_{41}Sn_{11}$ CNFs	0.469	1.07	3.951	16.84	$Cu_{4.262}Sn$ ($Cu_{4.3}Sn$)

Table S2. Distance between lattice plane of $Cu_{41}Sn_{11}$ (660), Cu_6Sn_5 (132), and Cu_6Sn_5 (-113) plane calculated from the theoretical model for DFT calculation and HRTEM analysis.

Plane	d-space of model (nm)	d-space from HRTEM (nm)
$Cu_{41}S_{11}$ (660)	0.212	0.210
Cu_6Sn_5 (132)	0.211	0.210
Cu_6Sn_5 (-113)	0.245	0.297

Table S3. The average FE and standard deviation for each CO_2RR product about CuO-SnO_2 NFs. These values were computed from three independent samples at each applied potential.

Products	Value (%)	-0.54 V (vs RHE)	-0.70 V (vs RHE)	-0.81 V (vs RHE)	-0.95 V (vs RHE)	-0.99 V (vs RHE)
H_2	Average FE	8.26	4.63	5.97	5.94	8.83
	Standard deviation	0.76	0.36	0.35	0.47	0.26
CO	Average FE	26.9	16.5	29.6	29.2	26.9
	Standard deviation	2.3	4.0	1.4	2.5	7.8
$HCOO^-$	Average FE	59.7	74.3	56.6	53.7	65.3
	Standard deviation	2.5	8.0	1.8	0.31	4.1

Table S4. The average FE and standard deviation for each CO_2RR product about Cu-SnO_2 NFs. These values were computed from three independent samples at each applied potential.

Products	Value (%)	-0.58 V (vs RHE)	-0.64 V (vs RHE)	-0.75 V (vs RHE)	-0.79 V (vs RHE)	-0.89 V (vs RHE)
H_2	Average FE	4.95	5.66	6.84	6.58	7.08
	Standard deviation	2.7	1.3	0.71	0.74	2.8
CO	Average FE	24.9	29.4	35.3	56.3	59.1
	Standard deviation	7.4	5.5	2.1	7.8	1.5
$HCOO^-$	Average FE	66.9	60.0	54.8	40.5	37.3
	Standard deviation	4.9	3.5	2.7	6.0	1.9

Table S5. The average FE and standard deviation for each CO_2RR product about Cu_3Sn/CNFs. These values were computed from three independent samples at each applied potential.

Products	Value (%)	-0.71 V (vs RHE)	-0.84 V (vs RHE)	-1.01 V (vs RHE)	-1.14 V (vs RHE)	-1.18 V (vs RHE)	-1.33 V (vs RHE)	-1.45 V (vs RHE)	-1.50 V (vs RHE)
H_2	Average FE	11.5	12.6	11.5	12	11.4	20.0	17.2	18.9
	Standard deviation	0.28	0.092	0.16	0.47	0.79	0.83	2.0	0.068
CO	Average FE	63.7	52.1	50.5	41.5	34.9	26.9	19.4	17.6
	Standard deviation	1.2	0.64	0.93	3.1	3.1	0.54	4.0	2.1
CH_4	Average FE	6.57	13.7	14.6	18.4	21.3	33.1	31.3	34.7
	Standard deviation	1.6	0.76	1.3	1.6	1.8	1.7	4.5	1.6
C_2H_4	Average FE	7.22	9.64	10.9	12.9	15.3	6.10	12.9	10.9
	Standard deviation	0.60	0.82	1.3	0.49	0.61	0.37	1.7	1.3
$HCOO^-$	Average FE	11.4	8.88	6.15	4.48	8.05	5.19	3.80	4.88
	Standard deviation	1.1	0.62	1.1	0.057	0.086	0.71	0.52	2.3
C_2H_5OH	Average FE	3.66	6.01	8.72	9.82	5.07	8.02	10.1	9.24
	Standard deviation	2.0	1.4	0.59	0.96	1.1	0.043	1.8	0.80
CH_3COO^-	Average FE	0.966	2.19	3.89	4.59	2.92	5.60	5.21	5.00
	Standard deviation	0.48	0.47	0.14	1.0	0.30	0.19	1.2	0.23

Table S6. The average FE and standard deviation for each CO_2RR product about $Cu_{41}Sn_{11}$/CNFs. These values were computed from three independent samples at each applied potential.

Products	Value (%)	-0.62 V (vs RHE)	-0.75 V (vs RHE)	-0.83 V (vs RHE)	-0.97 V (vs RHE)	-1.08 V (vs RHE)	-1.24 V (vs RHE)	-1.36 V (vs RHE)	-1.40 V (vs RHE)
H_2	Average FE	23.0	21.2	20.0	19.8	16.9	22.6	24.2	26.1
	Standard deviation	4.2	1.4	2.2	1.1	1.5	3.7	2.5	4.5
CO	Average FE	51.7	45.2	35.9	33.9	32.2	30.6	27.3	28.4
	Standard deviation	3.5	1.7	3.5	0.77	4.5	3.4	1.1	2.0
CH_4	Average FE	13.3	23.9	31.6	34.0	34.2	36.9	39.1	34.4
	Standard deviation	2.9	1.3	2.2	1.4	1.9	3.6	1.1	2.3
C_2H_4	Average FE	3.54	5.20	5.80	6.83	7.81	3.20	5.21	4.89
	Standard deviation	0.38	0.73	0.21	0.22	0.96	1.6	2.5	2.8
$HCOO^-$	Average FE	15.0	10.6	7.73	5.97	6.35	6.32	6.66	4.56
	Standard deviation	0.65	0.33	0.88	1.7	1.5	6.3	1.7	0.14
C_2H_5OH	Average FE	2.57	3.12	3.13	4.02	5.91	4.47	3.86	6.30
	Standard deviation	2.0	1.4	0.59	0.96	1.1	0.043	1.8	0.8
CH_3COO^-	Average FE	1.72	2.84	2.87	2.73	4.52	1.70	2.68	4.03
	Standard deviation	0.73	0.63	0.13	2.2	0.28	2.1	1.1	0.27

Table S7. The average FE and standard deviation for each CO_2RR product about Cu_6Sn_5/CNFs. These values were computed from three independent samples at each applied potential.

Products	Value (%)	-1.03 V (vs RHE)	-1.2 V (vs RHE)	-1.31 V (vs RHE)	-1.55 V (vs RHE)	-1.78 V (vs RHE)	-2.04 V (vs RHE)	-2.31 V (vs RHE)	-2.35 V (vs RHE)
H_2	Average FE	11.4	14.2	16.7	20.0	16.1	26.6	20.2	60.9
	Standard deviation	1.5	3.1	2.0	2.9	1.4	3.8	2.3	5.4
CO	Average FE	43.0	41.3	35.6	22.0	30.8	27.4	19.3	14.5
	Standard deviation	5.2	1.4	2.3	4.3	3.9	4.2	2.1	1.6
$HCOO^-$	Average FE	47.1	41.7	42.4	41.7	45.6	43.5	58.6	22.0
	Standard deviation	3.8	1.5	1.1	2.0	3.3	1.6	1.4	1.4

Reference

1. A. L. S. Eh, J. Chen, S. H. Yu, G. Thangavel, X. Zhou, G. Cai, S. Li, D. H. Chua and P. S. Lee, *Advanced Science*, 2020, **7**, 1903198.